

# Elastic $pp$ and $\bar{p}p$ scattering in the modified additive quark model

P. Desgrolard<sup>1,a</sup>, M. Giffon<sup>2,b</sup>, E. Martynov<sup>2,c</sup>

<sup>1</sup> Institut de Physique Nucléaire de Lyon, IN2P3-CNRS et Université Claude Bernard, 43 boulevard du 11 novembre 1918, 69622 Villeurbanne Cedex, France

<sup>2</sup> Bogoliubov Institute for Theoretical Physics, National Academy of Sciences of Ukraine, 03143, Kiev-143, Metrologicheskaja 14b, Ukraine

Received: 26 April 2000 / Revised version: 21 September 2000 /  
Published online: 8 December 2000 – © Springer-Verlag 2000

**Abstract.** The modified additive quark model, proposed recently, allows one to improve the agreement of the standard additive quark model with the data on the  $pp$ ,  $\bar{p}p$ ,  $\pi^\pm p$ ,  $\gamma p$  and  $\gamma\gamma$  total cross-sections, as well as on the ratios of real to imaginary part of the  $pp$  and  $\bar{p}p$  amplitudes at  $t = 0$ . Here, we extend this model to non-forward elastic scattering of protons and antiprotons. A high quality reproduction of the angular distributions at  $19.4 \text{ GeV} \leq s^{1/2} \leq 1800 \text{ GeV}$  is obtained. A zero at small  $|t|$  in the real part of the even amplitude in accordance with a recently proved general high energy theorem is found.

## 1 Introduction

Small angle elastic scattering of hadrons has always been a crucial source of information for the dynamics of the strong interaction. As a rule, these processes, being outside the realm of applications of the theory of the strong interactions (QCD), are described in approaches based on the  $S$ -matrix theory. In particular, the various Regge models are very successful at this point. However, in the framework of a Regge approach it is impossible to calculate all the ingredients needed in the amplitudes, and some additional arguments are used to construct main objects such as Regge trajectories and residue functions. Sometimes these are derived from the fundamental theory, but usually they are based on an intuitive physical picture and on the analysis of the available experimental data.

The additive quark model (AQM) [1] is an example of such a line of arguments. The amplitude of the composite particle interaction is constructed as a sum of the elementary amplitudes of the interaction among the constituent quarks. This leads to remarkable relations (counting rules) between the various hadronic cross-sections, in rather good agreement with the experimental data.

In a recent paper [2], the standard AQM (which we abbreviate in this old version as SAQM) and the ensuing counting rules are modified to take into account not only the quark–gluonic content of the pomeron but also of the secondary reggeons, as well as the fact that the soft pomeron is not just a gluonic ladder. The new model, which we call modified additive quark model (MAQM),

is successfully applied to describe various total cross-sections (nucleon–nucleon,  $\pi$  meson–nucleon,  $\gamma p$  and  $\gamma\gamma$ ) and the  $\rho$ -ratio of the real to the imaginary part of the forward  $pp$ ,  $p\bar{p}$  scattering amplitudes. The next step: to consider the differential cross-sections is the object of this paper, i.e. we extend and further test the model for  $t \neq 0$ . Let us recall that there are two couplings of the pomeron with quarks in MAQM: the first one corresponds to the ordinary vertex quark–pomeron–quark, another one is new and describes a “simultaneous” interaction of the pomeron with two quarks in a hadron. It was found from the fit to the cross-sections in [2] that the corresponding term in the amplitudes is negative. At some  $t \neq 0$  an interference of the ordinary and new term can produce a zero in the elastic amplitude and consequently a dip structure in the differential cross-section. This argument was one of reasons to extend MAQM for  $t \neq 0$ .

We deal only with  $pp$  and  $p\bar{p}$  elastic scattering because, for these processes, there are available the richest and most precise experimental data in a wide region of energy  $s^{1/2}$  and momentum transfer  $t$ . Many models (for instance [3–8]) of  $pp$  and  $p\bar{p}$  elastic scattering amplitudes describe quite well the available data (see also the reviews [9] and references therein). A supercritical pomeron with the intercept  $\alpha_P(0) > 1$  is used at the Born level for most of them [3–5]. Such a pomeron must then be unitarized because it does not satisfy the unitarity constraints. Usually the method of eikonalization [10] is used to reach this aim.

A method for reproducing the  $t \neq 0$  data, based on the model of the stochastic vacuum (attractive by its success), consists in parameterizing each angular distribution in the  $s, t$  space (see, for example, [8]), the energy de-

<sup>a</sup> e-mail: desgrolard@ipnl.in2p3.fr

<sup>b</sup> e-mail: giffon@ipnl.in2p3.fr

<sup>c</sup> e-mail: martynov@bitp.kiev.ua

pendence of the amplitude being absorbed in the parameters. The price to pay is of course the multiplication of the number of free parameters. An alternative way is to construct a model that from the beginning does not violate the requirements for the analyticity and unitarity of the scattering amplitude<sup>1</sup>. An example of such a model is the model of the so-called maximal pomeron and maximal odderon [6]. However, serious arguments against the maximal odderon exist [10,11].

In [2], we stick to the last kind of approach and we use an extended AQM which can be applied not only to nucleon–nucleon scattering. As an explicit choice, for the pomeron contribution we choose a simple model, namely a special case of the soft dipole pomeron, with a unit intercept [7,12] which leads to a high quality description of the experimental data, both at  $t = 0$  [13–16] and at  $t \neq 0$  (we show this in Sect. 4).

In the present paper we will not consider any eikonalization and work with the Born amplitudes since in the MAQM they do not violate unitarity (although with the restricted sense set above). However, it is not obvious that eikonalization should not be carried out since it corresponds to take into account the physical processes of rescattering corrections. We will not discuss this point here. The present work may be used as a guide for further investigations.

It should be stressed that the task of reproducing well the entire set of high energy data (at all values of the momentum transfer  $t$ ), though far from simple, as a long (and direct) experience teaches us, may seem to have a poor theoretical content [9]. This is indeed the truth in the sense that we have not yet any means of determining the soft amplitudes from first principles. However, we believe that it is important to explore all the approaches yielding a good agreement with the existing data. To the extent that these may lead to different extrapolations which, hopefully and foreseeably, will be checked in future experiments, we shall have a posteriori the means of establishing a hierarchy among them.

In Sect. 2, we recall the main assumptions of [2], focussing on a few arguments in favor of the chosen pomeron used in the MAQM at  $t = 0$ . In Sect. 3, we formulate our MAQM extension for  $t \neq 0$ . The results of the fit of the MAQM to the experimental data are presented and discussed in Sect. 4. We examine also if the amplitude that fits very well the data automatically exhibits a zero in the real part of its even component as required by a general theorem due to Martin [17]. Some items are also discussed in this section (concerning in particular the odderon and the logarithmic trajectories).

## 2 The modified additive quark model at $t = 0$

Let us review the main properties of the MAQM, formulated for the forward scattering amplitudes (for details see [2]).

<sup>1</sup> We mean only that the model should not violate grossly and explicitly the constraints of unitarity. This, unfortunately, does not guarantee that unitarity is satisfied

### 2.1 Pomeron

The pomeron contribution to the  $pp$  and  $\bar{p}p$  scattering amplitude at  $t = 0$  is written as<sup>2</sup>

$$A_{\mathcal{P}}^{(pp)}(s, 0) = 9P_{\mathcal{P}}^2[A_{\mathcal{P}}^{(1)}(s/9, 0) + 2A_{\mathcal{P}}^{(2)}(2s/9, 0) + A_{\mathcal{P}}^{(3)}(4s/9, 0)]. \quad (1)$$

The choice of the elementary pomeron quark–quark amplitudes  $A_{\mathcal{P}}^{(i=1-3)}$  is very important from a phenomenological point of view. It is known from a comparison of various pomeron models [13,16] that equivalent good fits to the  $t = 0$  data on the  $\rho$ -ratios of the real to imaginary parts of the forward amplitude  $\rho = \Re A(s, 0)/\Im A(s, 0)$  and on the total elastic cross-sections  $\sigma_{\text{tot}}$  for meson–nucleon and nucleon–nucleon interactions are achieved, at  $s \rightarrow \infty$ , either if  $\sigma_{\text{tot}} \propto \ln(s/s_0)$ , or  $\propto \ln^2(s/s_0)$  or  $\propto (s/s_0)^\epsilon$ . Unfortunately, as far as only  $pp$  and  $\bar{p}p$  are concerned, existing data do not allow one to discriminate unambiguously [14] between these three behaviors. Nevertheless, as noted in [16], the model with  $\sigma_{\text{tot}} \propto \ln(s/s_0)$  is the most “stable” in the sense that the fitted parameters and  $\chi^2/\text{d.o.f.}$  do not change in practice under variation of  $s_{\text{min}}$  in the energy range 5–10 GeV (the models were fitted to the data at  $s \geq s_{\text{min}}$ ).

Hence, among the possible pomerons, we select a “dipole pomeron” with an intercept equal to one,  $\alpha_{\mathcal{P}}(0) = 1$ , i.e. corresponding to a double pole of the amplitude in the complex angular momenta plane  $j$  and yielding an asymptotic behavior  $\sigma_{\text{tot}} \propto \ln(s/s_0)$  with an economy of parameters [16]. It is interesting to note that such a dipole pomeron is a singularity of the partial amplitude,  $\phi(j, t) \propto (j - \alpha_{\mathcal{P}}(t))^{-\gamma}$ , with the maximal hardness that does not violate the evident inequality  $\sigma_{\text{elastic}}(s) \leq \sigma_{\text{tot}}(s)$ . The inequality  $\gamma \leq 2$  must be satisfied if the pomeron trajectory at small  $t$  is linear,  $\alpha_{\mathcal{P}}(t) \approx 1 + \alpha'_{\mathcal{P}}t$ , and  $\gamma = 2$  corresponds to the dipole pomeron.

The contribution of the dipole pomeron to the forward hadron–hadron elastic scattering amplitude is written

$$A_{\mathcal{P}}^{\text{hh}}(s, 0) = C_1 + C_2 \ln(-is/s_0),$$

where  $C_1$ , as follows from the fit, is a negative constant (we consistently take  $s_0 = 1 \text{ GeV}^2$ ). This may be surprising because at small energies the contribution of the dipole pomeron to  $\sigma_{\text{tot}}$  would be negative<sup>3</sup>. However, this term can be treated [18] as an effective contribution of the pomeron rescatterings and it is straightforward to demonstrate that its sign may be negative. The above arguments and those given in [2] suggest that we may choose to write the pomeron amplitudes in MAQM at  $t = 0$  as follows:

$$\begin{aligned} A_{\mathcal{P}}^{(1)}(s, 0) &= ig_1^2[-\zeta_{\mathcal{P}} + L(s)], \\ A_{\mathcal{P}}^{(2)}(s, 0) &= ig_1g_2[-\zeta_{\mathcal{P}} + L(s)], \\ A_{\mathcal{P}}^{(3)}(s, 0) &= ig_2^2[-\zeta_{\mathcal{P}} + L(s)], \end{aligned} \quad (2)$$

<sup>2</sup> The pomeron contributions to the  $\pi p, \gamma p$  and  $\gamma\gamma$  amplitudes are given in [2]

<sup>3</sup> This is noted also in [16]

where

$$L(s) = \ln(-is/s_0).$$

## 2.2 Secondary reggeons

In  $pp$  and  $\bar{p}p$  scattering, the secondary reggeons are numerous; however, for the energy range involved here we can choose to keep only  $f$  and  $\omega$  reggeons, two non-degenerate  $C = +1$  and  $C = -1$  meson trajectories. As is argued in [2] instead of nine identical diagrams for the  $f$  reggeon in the SAQM, leading to the factor 9, one obtains

$$A_f^{(pp)}(s, 0) = P_p^2(5 + 4\lambda_f)A_f^{(qq)}(s/9, 0), \quad (3)$$

where

$$A_f^{(qq)}(s, 0) = ig_f^2(-is/s_0)^{\alpha_f(0)-1} \quad (4)$$

and  $\lambda_f$  is a constant taking into account a mixing of  $u\bar{u}$  and  $d\bar{d}$  quark states in the  $f$  reggeon. Similarly, for the  $\omega$  reggeon we set

$$A_\omega^{(pp)}(s, 0) = P_p^2(5 + 4\lambda_\omega)A_\omega^{(qq)}(s/9, 0), \quad (5)$$

$$A_\omega^{(qq)}(s, 0) = g_\omega^2(-is/s_0)^{\alpha_\omega(0)-1}. \quad (6)$$

An important property of the dipole pomeron model is that all fits give a high value of the  $f$  reggeon intercept,  $\alpha_f(0) \approx 0.80 \div 0.82$  [13–16]. Does such an intercept contradict the data on the  $f$  trajectory known from the resonance region? The answer is “yes” if the trajectory is assumed to be linear. However, aside from general theoretical arguments against linear trajectories, the experimental data on the resonances lying on the  $f$  trajectory indicate its non-linearity (see Fig. 1).

The following parabola passes exactly through the three known resonances:  $\alpha_f(t) = \alpha_f(0) + \alpha'_f t + \beta_f t^2$  with  $\alpha_f(0) = 0.96$ ,  $\alpha'_f = 0.59 \text{ GeV}^{-2}$ ,  $\beta_f = 0.03 \text{ GeV}^{-4}$ . This leads to a too high intercept and can cause problems in the fit to differential cross-sections at large  $|t|$ . A more realistic trajectory such as  $\alpha_f(t) = \alpha_f(0) + \gamma_1((4m_\pi^2)^{1/2} - (4m_\pi^2 - t)^{1/2}) + \gamma_2((t_1)^{1/2} - (t_1 - t)^{1/2})$  gives  $0.77 < \alpha_f(0) < 0.87$ .

Generally, there is an evident correlation between the intercept of the  $f$  reggeon and the model for the pomeron. This is due to the fact that in all known processes, pomeron and  $f$  reggeon contribute additively. As a rule, a higher  $f$  intercept is associated with a slower growth with energy due to the pomeron contribution (as an example see also [16]). In Fig. 2, we illustrate this observation and show how  $\alpha_f(0)$  is correlated with a power of  $\ln s$  in the behavior of the total cross-section, if the forward scattering amplitudes are parameterized in the form

$$A^{\text{hh}}(s, 0) = i[C_1 + C_2 \ln^\gamma(-is/s_0)] + R(s, 0),$$

where the explicit form of the secondary reggeon contribution  $R(s, 0)$ , depends on the nature of the interacting hadrons (see [13, 16] for details).

In our opinion, a good way to fix the intercepts of  $f$  and  $\omega$  reggeons is after fitting the total cross-sections.

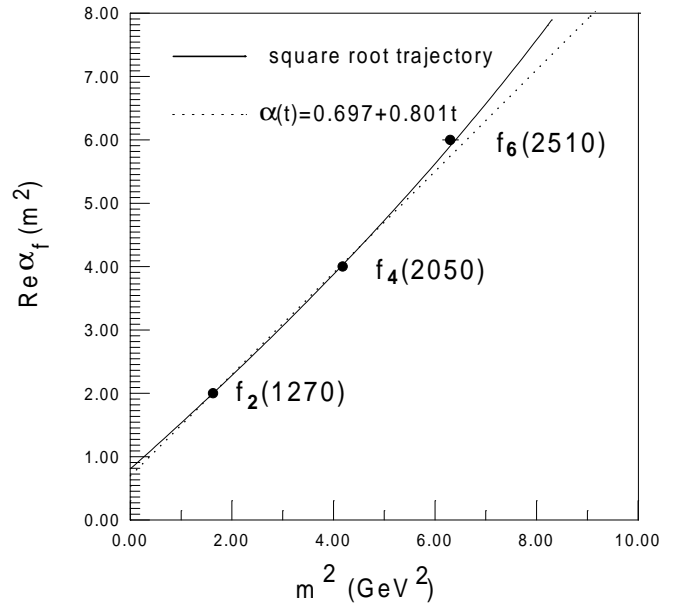


**Fig. 1.** Real part of the  $f$  trajectory versus  $m^2$ , the squared mass of the resonance. The solid line is the square-root trajectory used in the present work (see the text). The dashed straight line is the result of a linear fit

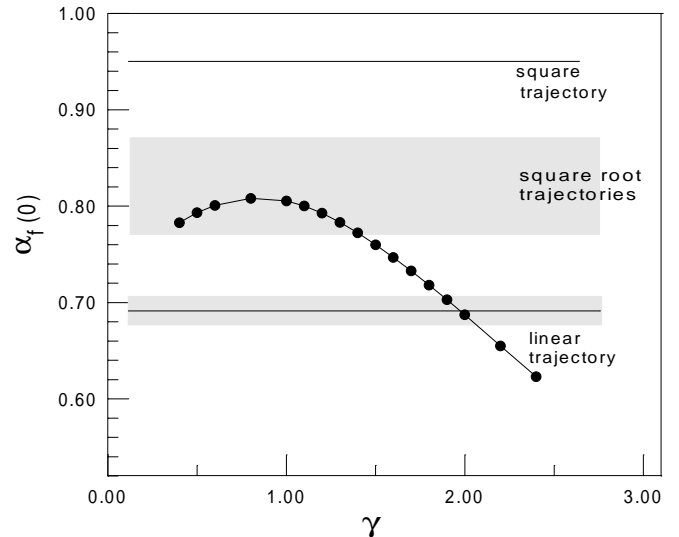


**Fig. 2.** Intercept of the  $f$  trajectory correlated with the power  $\gamma$  of  $\ln s$  in  $\sigma_{\text{tot}}(s)$ . Intervals for an intercept of various parameterizations are shown

Doing so and avoiding an extra number of parameters, we choose the following form of the  $f$  trajectory:

$$\alpha_f(t) = \alpha_f(0) + \gamma_f(\sqrt{t_f} - \sqrt{t_f - t}),$$

where the intercept  $\alpha_f(0) = 0.810$  is fixed from the fit [2] to the total cross-sections, the effective threshold  $t_f = 14.964 \text{ GeV}^2$  and the parameter  $\gamma_f = 5.504 \text{ GeV}^{-1}$  are determined from the fit to the positions of the three known resonances.

For the  $\omega$  trajectory (with only two known resonances and absence of information on possible higher resonances) we use a linear form,

$$\alpha_\omega(t) = \alpha_\omega(0) + \alpha'_\omega t,$$

with the intercept  $\alpha_\omega(0) = 0.422$  from [2] and with the slope  $\alpha'_\omega = 0.946 \text{ GeV}^{-2}$  determined in a fit to the resonances.

### 3 The modified additive quark model at $t \neq 0$

The amplitudes of interest are written

$$A_{pp}^{\bar{p}p}(s, t) = A_{\mathcal{P}}(s, t) + A_f(s, t) \pm [A_{\mathcal{O}}(s, t) + A_\omega(s, t)]. \quad (7)$$

The normalization is

$$\sigma_{\text{tot}}(s) = 8\pi \Im m A(s, t=0), \quad \frac{d\sigma}{dt}(s, t) = 4\pi |A(s, t)|^2. \quad (8)$$

The starting points for a parameterization of all terms in (7) at  $t \neq 0$  are the corresponding partial amplitudes defined at  $t = 0$  in [2] and rewritten in detail in (1)–(6). A special discussion will be devoted to the odderon amplitude  $a_{\mathcal{O}}(s, t)$  which is out of the game at  $t = 0$ .

Let us recall that, in accordance with the main assumption of the additive quark model (as well as of MAQM [2]), there is an interaction of two (in fact of  $3 \times 3$ ) constituent quarks (or lines in terms of a diagram), each of them carrying only a part of the momentum  $\mathbf{p}$ . Therefore, we must define  $s_q = (p_1 + p_2)^2 = s/9$ , for protons, assuming that the whole momentum is distributed equally between all quarks in each of them. As concerns the  $t$  channel, we consider for pomeron and  $f$  reggeon a single exchange (one line in the  $t$  channel in terms of a diagram); our odderon also is supposed to behave as a one reggeon exchange. Consequently, we have no reason to divide  $t$  in the final amplitude by any number<sup>4</sup>.

#### 3.1 Pomeron

Starting from (1), the pomeron contribution at  $t \neq 0$  will have the form

$$A_{\mathcal{P}}(s, t) = 9[A_{\mathcal{P}}^{(1)}(s/9, t) + 2A_{\mathcal{P}}^{(2)}(2s/9, t) + A_{\mathcal{P}}^{(3)}(4s/9, t)]. \quad (9)$$

The most direct generalization of  $A_{\mathcal{P}}^{(i=1-3)}(s, 0)$  (in (2)) is to consider all “coupling constants”  $g_1, g_2, \zeta_{\mathcal{P}}$  as functions of  $t$  and to multiply each  $A_{\mathcal{P}}^{(i)}(s, 0)$  by the usual Regge factor  $(-is/s_0)^{\alpha_{\mathcal{P}}(t)-1}$ . Namely, we write

$$\begin{aligned} A_{\mathcal{P}}^{(1)}(s, t) &= ig_1^2(t)[- \zeta_{\mathcal{P}}(t) + L(s)](-is/s_0)^{\alpha_{\mathcal{P}}(t)-1}, \\ A_{\mathcal{P}}^{(2)}(s, t) &= ig_1(t)g_2(t)[- \zeta_{\mathcal{P}}(t) + L(s)] \\ &\quad \times (-is/s_0)^{\alpha_{\mathcal{P}}(t)-1}, \\ A_{\mathcal{P}}^{(3)}(s, t) &= ig_2^2(t)[- \zeta_{\mathcal{P}}(t) + L(s)](-is/s_0)^{\alpha_{\mathcal{P}}(t)-1}. \end{aligned} \quad (10)$$

<sup>4</sup> Such a division, e.g. by 9, occurs when three gluon or three pomeron exchanges (three lines in  $t$  channel) are considered (as in [19]), implying a distribution of the momentum  $\mathbf{q}$  along three lines, each of them being assumed to carry an averaged momentum  $\mathbf{q}/3$

As the simplest variant we choose the linear pomeron trajectory (again with an intercept equal to 1)

$$\alpha_{\mathcal{P}}(t) = 1 + \alpha'_{\mathcal{P}} t; \quad (11)$$

we consider also the case of a logarithmic trajectory which is discussed in details in Sect. 4.

Of course, more sophisticated pomeron models can be proposed, but these lead to an extra number of parameters and we will not consider them. Finally, to avoid proliferation of parameters, we will assume simple exponential “residue functions”  $g_{i=1,2}$  and  $\zeta_{\mathcal{P}}$ :

$$\begin{aligned} g_1(t) &= g_1 \exp(b_1 t), \quad g_2(t) = g_2 \exp(b_2 t), \quad \zeta_{\mathcal{P}}(t) \\ &= \zeta_{\mathcal{P}} \exp(b_{\zeta_{\mathcal{P}}} t). \end{aligned} \quad (12)$$

Thus there are seven ( $g_1, g_2, \zeta_{\mathcal{P}}, b_1, b_2, b_{\zeta_{\mathcal{P}}}, \alpha'_{\mathcal{P}}$ ) parameters for the pomeron term of the amplitude. With this pomeron model the Froissart–Martin bound is not violated and the total cross-section behaves as  $\ln s$  when  $s \rightarrow \infty$ .

#### 3.2 Secondary reggeons

Generalizing [2], the  $f$  reggeon amplitude in the MAQM is written as

$$A_f(s, t) = (5 + 4\lambda_f) A_f^{(qq)}(s/9, t), \quad (13)$$

where

$$\begin{aligned} A_f^{(qq)}(s, t) &= ig_f^2 \left( -i \frac{s}{s_0} \right)^{\alpha_f(t)-1} e^{b_f t}, \\ \alpha_f(t) &= \alpha_f(0) + \gamma_f (\sqrt{t_f} - \sqrt{t_f - t}). \end{aligned} \quad (14)$$

As already noted above, for that  $f$  reggeon trajectory we choose a square-root dependence on  $t$ , which is more suitable than a linear one, and fix its parameters from the fits to cross-sections and resonances (see Sect. 2.2). The value of  $\lambda_f$  is unimportant if only  $pp$  and  $\bar{p}p$  processes are considered (this is equivalent to the redefinition of the coupling  $g_f$ ). Nevertheless, for the present work we keep  $\lambda_f = 0.439$  which was obtained from the fit at  $t = 0$  (see [2]). The number of free parameters for a fixed trajectory is then only two ( $g_f, b_f$ ).

Following the previous considerations, we write for the  $\omega$  reggeon

$$A_\omega(s, t) = (5 + 4\lambda_\omega) A_\omega^{(qq)}(s/9, t), \quad (15)$$

where

$$\begin{aligned} A_\omega^{(qq)}(s, t) &= g_\omega^2 \left( -i \frac{s}{s_0} \right)^{\alpha_\omega(t)-1} e^{b_\omega t}, \\ \alpha_\omega(t) &= \alpha_\omega(0) + \alpha'_\omega t. \end{aligned} \quad (16)$$

For the  $\omega$  reggeon trajectory, we recall that we choose a linear dependence on  $t$ , with the parameters given in Sect. 2.2.

In [12] a multiplicative factor  $r_\omega(s, t)$  was introduced in  $A_\omega^{(qq)}(s, t)$  to describe the so-called ‘‘cross-over phenomenon’’, namely, a zero at small  $t$  in the difference of the  $\bar{p}p$  and  $pp$  differential cross-sections. Here, we extend the kinematic region under consideration up to  $|t| \approx 14 \text{ GeV}^2$  and also include odderon contributions. An interference of various odd terms in amplitude now could produce the mentioned zero automatically and thus we set  $r_\omega(s, t) = 1$ . Again, repeating the arguments given above for the  $f$  reggeon, we put  $\lambda_\omega = 1$ . When the trajectory is fixed, we are left with only two free parameters ( $g_\omega, b_\omega$ ).

### 3.3 Odderon

This crossing-odd contribution (added to the  $\omega$  reggeon) is a quite delicate and ambiguous point, lacking sufficiently precise and numerous data. A widespread consensus [13, 14, 16], however, is that an odderon contribution while insignificant at  $t = 0$  is very relevant in the large  $|t|$  domain.

As compared with the previous contributions, it is important to notice that it is impossible to apply to the odderon any additive quark model rule. The odderon, in contrast with the pomeron and secondary reggeons, interacts with the whole proton rather than with separate quarks since three gluons (or the odderon according to Donnachie and Landshoff [20]) couple simultaneously with three quarks in each  $p$  or  $\bar{p}$ .

As repeatedly mentioned, in this paper we stick to the Born approximation and rescattering corrections are not taken into account. This is known to be inadequate from the conceptual point of view and not just for practical reasons of restoring unitarity when the Born approximation leads to its violation. The point is particularly delicate concerning the odderon which, by universal consensus, should be important at large  $|t|$ . For this reason, we parameterize the odderon, somewhat artificially, as the sum of two contributions which we denote as ‘‘soft’’ and ‘‘hard’’:

$$A_{\mathcal{O}}(s, t) = A_{\mathcal{O}}^{(s)}(s, t) + A_{\mathcal{O}}^{(h)}(s, t). \quad (17)$$

As is known, the contribution of odderon at  $t = 0$  is negligible. We take into account this fact multiplying both components by a factor vanishing at  $t = 0$ . For the soft odderon we assume like for the pomeron a dipole form, suitably damped<sup>5</sup>

$$A_{\mathcal{O}}^{(s)}(s, t) = g_{\mathcal{O}s}(t) [(1 - e^{\beta_s t}) \ln(-is/s_0)]^\mu \times [-\zeta_{\mathcal{O}s}(t) + \ln(-is/s_0)] \left(-i \frac{s}{s_0}\right)^{\alpha_{\mathcal{O}}(t)-1}, \quad (18)$$

while for the hard one, we choose

$$A_{\mathcal{O}}^{(h)}(s, t) = g_{\mathcal{O}h}(1 - e^{\beta_h t}) [\ln(-is/s_0)]^\nu \frac{1}{(1 - t/t_{\mathcal{O}h})^4}. \quad (19)$$

We should give here a few comments concerning the choice of the odderon amplitude defined by the above equations.

<sup>5</sup> Strictly speaking it has dipole form only if  $\mu = 0$

- (1) The contribution of the soft odderon to  $\sigma_{\text{elastic}}$  is dominated by the region where  $|t|$  is small. In this domain the factor  $(1 - e^{\beta_s t}) \ln(-is/s_0)$  is nearly constant. This means that the soft odderon does not violate the evident inequality  $\sigma_{\text{elastic}} \leq \sigma_{\text{tot}}$  at any value of  $\mu$ .
- (2) At the same time the amplitude should not have a singularity at  $t = 0$ ; therefore  $\mu$  must be an integer. In the fits we have considered  $\mu = 1$  and  $\mu = 2$ .
- (3) The hard odderon does not exponentially decrease with  $|t|$ , therefore it does not violate the restriction  $\sigma_{\text{elastic}} \leq \sigma_{\text{tot}}$  at any  $s$  only if  $\nu \leq 1/2$ .
- (4) We consider a linear odderon trajectory but with a non-unit intercept, only constrained by unitarity<sup>6</sup>:

$$\alpha_{\mathcal{O}}(t) = 1 + \delta_{\mathcal{O}} + \alpha'_{\mathcal{O}} t, \quad \delta_{\mathcal{O}} \leq 0. \quad (20)$$

In fact, as will be emphasized below, only the upper bound of the intercept may be kept.

- (5) As for the pomeron, the soft residue functions are taken in an ordinary exponential form

$$g_{\mathcal{O}s}(t) = g_{\mathcal{O}s} e^{b_{\mathcal{O}} t}, \quad \zeta_{\mathcal{O}s}(t) = \zeta_{\mathcal{O}} e^{b_{\zeta_{\mathcal{O}}} t}. \quad (21)$$

The case of a logarithmic trajectory is reserved for discussion. Thus the odderon contribution is controlled by a maximum of ten additional parameters:  $g_{\mathcal{O}s}, \zeta_{\mathcal{O}}, \beta_s, b_{\mathcal{O}}, b_{\zeta_{\mathcal{O}}}, \delta_{\mathcal{O}}, \alpha'_{\mathcal{O}}, g_{\mathcal{O}h}, t_{\mathcal{O}h}, \beta_h$ .

The grand total number of free parameters for MAQM is twenty-six; however, this number will be reduced by fixing some of them by virtue of special arguments. For example, this paper being devoted to  $pp$  and  $\bar{p}p$  angular distributions, all coupling constants and intercepts are fixed from the fit to  $\sigma_{\text{tot}}$  and  $\rho$  at  $t = 0$  as reported in [2]; furthermore, the remaining parameters of the reggeon trajectories are fixed here from the resonances; not excluding simplifications in the chosen form for the odderon.

## 4 Results and discussion

### 4.1 Previous results at $t = 0$

It is our choice to extract from [2] the informations useful for  $pp$  and  $\bar{p}p$  at  $t = 0$ . Of course, we do not claim that better fits are not possible for forward scattering; many very good old and recent parameterizations beyond our scope in the present discussion are available for  $pp$  and  $\bar{p}p$  processes. Thus, as a first step, we refer to the results found in [2], where 217  $t = 0$  data (for  $pp$  and  $\bar{p}p$ ) with  $4 \text{ GeV} \leq s^{1/2} \leq 1800 \text{ GeV}$  [21] have been taken into account, within combined fits of the  $pp, \bar{p}p, \pi^- p, \pi^+ p, \gamma\gamma, \gamma p$  total cross-sections and  $\rho$ -ratios. The selected results of interest here are given in Table 1, which exhibits the improvement brought to the old AQM by the modifications called in the revisited AQM. The  $\chi^2/\text{d.o.f.}$  (for all processes) was 1.78 in the MAQM (recall that we fitted our model to the data at  $s^{1/2} \geq 4 \text{ GeV}$  instead of  $s^{1/2} \geq 5 \text{ GeV}$

<sup>6</sup> For a discussion of a possible intercept less than one for the odderon, see for example [10] and references therein

**Table 1.** The partial  $\chi^2$ s obtained by fitting at  $t = 0$  [2] in the SAQM (old) and the MAQM (modified)

| Observable       | $\sigma_{\text{tot}}^{pp}$ | $\sigma_{\text{tot}}^{\bar{p}p}$ | $\rho^{pp}$ | $\rho^{\bar{p}p}$ |
|------------------|----------------------------|----------------------------------|-------------|-------------------|
| Number of points | 85                         | 51                               | 64          | 17                |
| $\chi^2$ SAQM    | 220                        | 240                              | 157         | 17                |
| $\chi^2$ MAQM    | 53                         | 59                               | 147         | 18                |

in [13,16]). The recalculated  $\chi^2/\text{d.o.f.}$  (specifically for  $pp$ ,  $\bar{p}p$  processes) is 1.32 in the MAQM. The corresponding behaviors of  $\sigma_{\text{tot}}(s)$  and of  $\rho(s) = \Re A(s,0)/\Im m A(s,0)$  are plotted in [2]. To complete the discussion, we give in Table 2 the parameters issued from the combined fits in [2], used here for the  $pp$  and  $\bar{p}p$  processes.

#### 4.2 MAQM results at $t \neq 0$

The previous seven parameters are kept fixed to their values determined by the  $t = 0$  combined fits. In addition, we fixed from fits to the resonances those parameters of the reggeon trajectories that are relevant at  $t \neq 0$ . Their determination in the present work is recalled in Table 3 (see also Sect. 2.2).

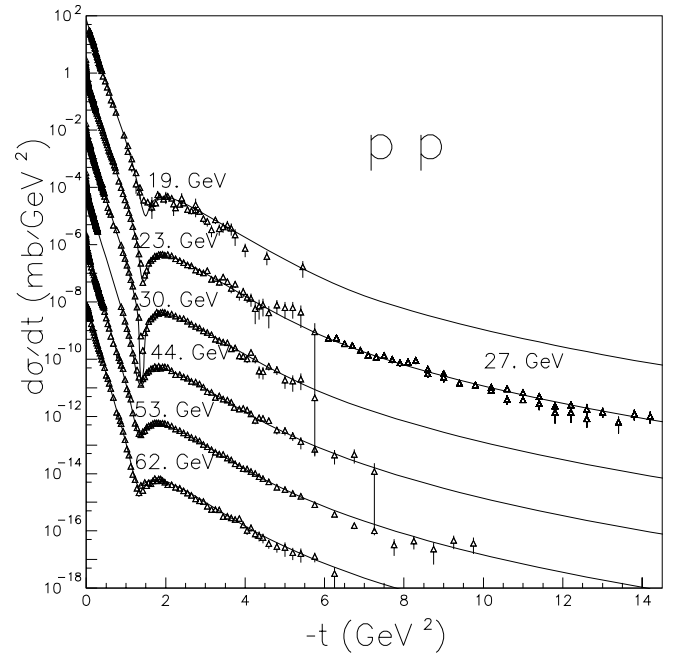
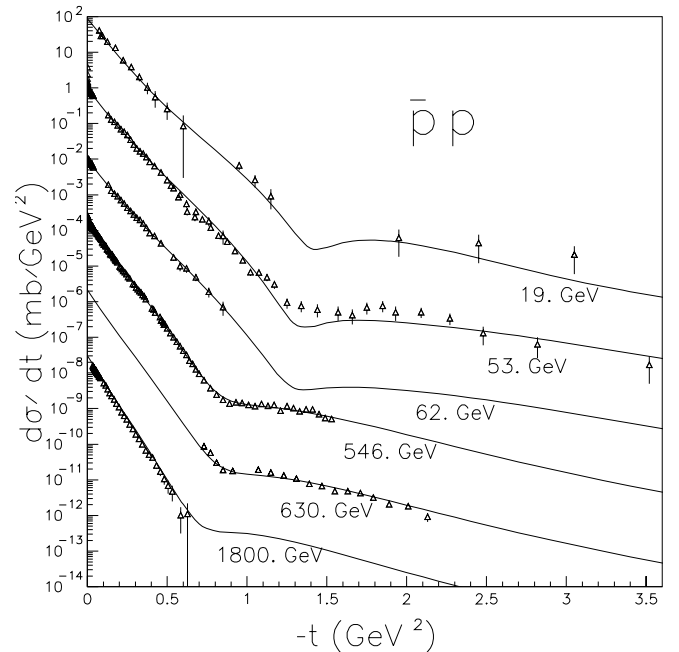
Only the remaining parameters are fitted in isolation from the angular distributions. Of course, the final  $\chi^2$  could be improved by refitting the complete set of parameters for the  $pp$  and  $\bar{p}p$  processes alone, but we decide against doing so. In this second step, we account for 959  $t \neq 0$  data [21] with  $0.1 < |t|$  ( $\text{GeV}^2$ )  $\leq 14.2$ ;  $19.4 \leq s^{1/2}$  ( $\text{GeV}$ )  $\leq 630$ . The selection  $|t| > 0.1 \text{ GeV}^2$  is used in order to exclude the Coulomb–nuclear interference region. It could be included as a refinement.

After preliminary trials, we select the following conditions for the current parameterization:

- (i)  $\mu = 2$  is chosen here because it gives a slightly better  $\chi^2$ , but taking  $\mu = 1$  does not influence significantly the quality of the fit: once more the data do not seem precise enough to select a specific form of the odderon;
- (ii)  $\nu = 1/2$ : for this (maximal) value, the odderon does not violate unitarity, the results at high energy (LHC) do not seem abnormal and the odderon can be considered as an effective phenomenological contribution;
- (iii) one may fix without damaging the results a unit intercept for the odderon ( $\delta_{\mathcal{O}} = 0$ ) as for our pomeron and in agreement with [22];
- (iv) linear trajectories are used throughout (except for the  $f$ ), which represents the more economic (if not the more efficient) solution;
- (v) furthermore, as unitarity requires [23], we constrained  $\alpha'_{\text{od}} \leq \alpha'_p$ .

We found the results distributed according to Table 4.

The corresponding  $\chi^2/\text{d.o.f.}$  (for  $t \neq 0$ ) is 2.38 (for 959 data and 15 parameters listed in Table 5) and recalculated with the  $t = 0$  and  $t \neq 0$  data together (with the couplings and intercepts given in Table 2) is 2.19 (for 1176 data and 22 parameters).

**Fig. 3.** Fit of the differential cross-sections of the  $pp$  interaction, calculated in MAQM. A factor  $10^{-2}$  between each successive energy is omitted**Fig. 4.** The same as in Fig. 3, for  $\bar{p}p$ . The Tevatron data are not fitted

We found, within the MAQM, a pretty good reproduction of the data (including the dip and the high  $|t|$  regions), exhibited in Figs. 3 and 4.

Searching for an improvement of our results (and accepting to “measure” the quality of a model by the  $\chi^2/\text{d.o.f.}$  because we have nothing better), as already said, it is possible to get a better agreement with the data when refitting all the parameters together to the forward and

**Table 2.** Values of the parameters controlling the MAQM amplitudes at  $t = 0$  [2]. Recall that the pomeron intercept equals 1, and the values quoted for  $g_f$  and  $g_\omega$  are coupled to  $\lambda_f = 0.439$  and  $\lambda_\omega = 1$ , respectively

| Parameter     | $g_1$ (GeV $^{-1}$ ) | $g_2$ (GeV $^{-1}$ ) | $\zeta_P$ | $g_f$ (GeV $^{-1}$ ) | $\alpha_f(0)$ | $g_\omega$ (GeV $^{-1}$ ) | $\alpha_\omega(0)$ |
|---------------|----------------------|----------------------|-----------|----------------------|---------------|---------------------------|--------------------|
| Value in MAQM | 0.3166               | -0.0239              | 3.396     | 1.112                | 0.8100        | 0.3948                    | 0.4217             |

**Table 3.** Values of the parameters driving the reggeon trajectories at  $t \neq 0$ , determined by fitting the resonances

| Reggeon trajectory | “f”<br>square-root (14)         | “ $\omega$ ”<br>linear (16) |  |
|--------------------|---------------------------------|-----------------------------|--|
| number of data     | 3 resonances                    | 2 resonances                |  |
| parameter          | $\gamma_f$<br>5.504 GeV $^{-1}$ | $t_f$<br>14.964 GeV $^2$    | $\alpha'_\omega$<br>0.9459 GeV $^{-2}$ |

**Table 4.** The partial  $\chi^2$  obtained by fitting the angular distributions in the MAQM with the parameters in Table 5

| Observable       | $(d\sigma/dt)^{pp}$ | $(d\sigma/dt)^{\bar{p}p}$ |
|------------------|---------------------|---------------------------|
| Number of points | 758                 | 201                       |
| $\chi^2$         | 1636                | 616                       |

**Table 5.** Parameters of MAQM obtained in fitting the angular distributions

|                  |   |               |
|------------------|---|---------------|
| Pomeron          | $b_1$ , GeV $^{-2}$                     | .1975E+01     |
|                  | $b_2$ , GeV $^{-2}$                     | -.2121E+00    |
|                  | $b_{\zeta_P}$ , GeV $^{-2}$             | .1227E+01     |
|                  | $\alpha'_{\mathcal{P}}$ , GeV $^{-2}$   | .3308E+00     |
| $f$ reggeon      | $b_f$ , GeV $^{-2}$                     | .4094E+01     |
| $\omega$ reggeon | $b_\omega$ , GeV $^{-2}$                | $\approx 0.0$ |
| Odderon (soft)   | $g_{\mathcal{O}s}$ , GeV $^{-2}$        | -.1305E-02    |
|                  | $\zeta_{\mathcal{O}}$                   | .2234E+02     |
|                  | $\beta_s$ , GeV $^{-2}$                 | .5023E+01     |
|                  | $b_{\mathcal{O}}$ , GeV $^{-2}$         | -.1693E+00    |
|                  | $b_{\zeta_{\mathcal{O}}}$ , GeV $^{-2}$ | .1417E+01     |
|                  | $\alpha'_{\mathcal{O}}$ , GeV $^{-2}$   | .3208E+00     |
| Odderon (hard)   | $g_{\mathcal{O}h}$ , GeV $^{-2}$        | .2434E+01     |
|                  | $t_{\mathcal{O}h}$ , GeV $^2$           | .4137E+00     |
|                  | $\beta_h$ , GeV $^{-2}$                 | .1197E+01     |

non-forward observables, for  $pp$  and  $\bar{p}p$  only. In that case, we find only a non-significant improvement in the sense that no modifications are seen on the figures. Any significant improvement of the  $\chi^2$  is not automatically followed by an improvement visible on the curves.

It is of some interest to compare our results with those of other approaches. A strict comparison is not easy because, if many of them are available, they present different objectives, and it is not our aim to discuss the relative virtues and shortcomings of each work. The model of [8] for example is an eikonalized model, not operating at the

**Table 6.** First values of  $-t$  cancelling  $\Re e A^+(s, t)$  and  $\Re e A_{\mathcal{P}}(s, t)$ , versus the energy, obtained in the MAQM fit

| Energy (GeV) | zero of $\Re e A^+$<br>$-t$ (GeV $^2$ ) | zero of $\Re e A_{\mathcal{P}}$<br>$-t$ (GeV $^2$ ) |
|--------------|---|---|
| 546          | 0.31                                    | 0.37  |
| 1800         | 0.27                                    | 0.29  |
| 10000        | 0.21                                    | 0.22  |
| 14000        | 0.21                                    | 0.22  |

Born level like ours, in which the energy dependence of the amplitude is absorbed in the parameters. At the Born level, the nearest models are probably the old models of [20,6], based on the Regge theory; furthermore, their results are grossly comparable to ours. The first one contains in particular a two pomeron exchange and contributions of other cuts which are absent in our approach. The second one involves a large number of parameters and the data at high  $|t|$  are not correctly reproduced.

### 4.3 Unitarity, odderon and logarithmic trajectories

#### 4.3.1 $\Re e A^+(s, t)$

As a by-product of the present study, we propose to consider the scattering amplitude obtained in our MAQM from the point of view of unitarity and analyticity. To be specific we want to insure that this amplitude not only respects the Froissart–Martin bound but also exhibits a zero at low  $|t|$  in  $\Re e A^+(s, t)$ , the real part of its even contribution (with respect to the  $C$ -parity), as required by a high energy theorem recently stated by Martin [17].

The situation of the first zero of  $\Re e A^+(s, t)$  is shown in Table 6 for some selected high energies. We agree with the theorem, with the results quoted in [17] and some of the extensive discussion [8] exhibiting in particular a first zero of the real part at low  $|t|$ , decreasing monotonically with the energy.

By also reporting  $\Re e A_{\mathcal{P}}(s, t)$  in Table 6, we exhibit a manifestation of the dominance of the pomeron at high energies, when the  $f$  reggeon contribution becomes negligible above the ISR energy range.

#### 4.3.2 $\Im m A^+(s, t)$

$\Im m A^+(s, t)$ , the imaginary part of the even component of the amplitude, has an oscillatory behavior for large

$|t|$ , in spite of lacking any rescattering corrections in the model. This is a consequence of the negative sign of the new MAQM (comparing with the old SAQM) coupling constant  $g_2$  (see Table 2). Oscillations, or something appearing as diffraction-like secondary structures, are hidden in the differential cross-sections because of the odderon contribution dominating in this domain. Of course our present MAQM model cannot produce any oscillations at large  $|t|$ , because it is a model at the Born approximation level, in which the odderon dominates at very high energy and in the high  $|t|$  region with a  $\sim 1/t^4$  behavior of the amplitude (see (19)). As a next step, it would be interesting to eikonalize the model to see in particular if oscillations in  $d\sigma/dt$  appear. We believe that rescattering corrections (we plan to calculate them in the near future) may be important at such high energies as will be investigated for instance in the TOTEM and PP2PP projects (see for example [24]), and as a consequence any extrapolation (in particular those of the angular distributions) may be doubtful within the present version of the non-eikonalized MAQM model.

#### 4.3.3 Logarithmic trajectories

As already mentioned above, the “hard” component of the odderon with a power behavior at large  $|t|$  looks affected from the point of view of the Regge approach (note here that for the whole set of data the ratio  $|t|/s$  is small, and we are in the domain of small angle scattering, that, we believe, should be described by Regge theory while the hard odderon component can be important at larger  $|t|$ ).

Taking into account the above argument we have considered the model without its “hard” odderon component, but for the pomeron and the (soft) odderon we have tested the non-linear trajectories with a logarithmic behavior:

$$\alpha_i(t) = 1 + \gamma_i [1 - (1 - t_i/t) \ln(1 - t/t_i)], \quad i = \mathcal{P}, \mathcal{O}. \quad (22)$$

The minimal value of the threshold  $t_{\mathcal{P}}$  (there are many thresholds in the  $t$  channel for  $pp$  and  $\bar{p}p$ ) should be given by the  $t$  channel physical state with the minimal mass (in our case a two-pion state, so  $t_{\mathcal{P}}^{\min} = 4m_{\pi}^2$ ). Nevertheless, in order to take into account the influence of other thresholds we consider  $t_{\mathcal{P}}$  as a free (effective) parameter. A similar argument can be repeated for the odderon trajectory.

Logarithmic trajectories mimic a power decreasing amplitude with  $|t| \rightarrow \infty$ . However, in order to give a meaning to such a possibility, it is necessary to replace the exponential residue functions by power ones. This leads to an extra number of free parameters. Therefore we used another, probably oversimplified, method. All exponents,  $\exp(b_i t)$  in the pomeron and in the soft odderon terms are replaced by  $\exp[(\alpha_{\mathcal{P}(\mathcal{O})}(t) - 1)b_i]$ . Using logarithmic trajectories, we do not aim to obtain the best fit; rather we only want to check our belief (and to demonstrate for the reader) that it is then possible to reproduce the large  $|t|$  data.

The resulting  $\chi^2/\text{d.o.f.} = 3.39$  as well as the agreement with the data is not so bad. The calculated angular

distributions slightly deviate from the data points mainly around the dips for  $pp$  but, as we expected, are very well reproduced for the large  $|t|$  domain.

#### 4.3.4 Conclusion

Summarizing, we emphasize that the obtained results confirm and reinforce the conclusion of [2] as a further test of the model: taking account of the corrections to the pomeron–quark interaction and obtaining new counting rules for the secondary reggeons. In other words using the modified additive quark model instead of the standard additive quark model leads to a good agreement with the available experimental data not only at  $t = 0$ , but also at  $t \neq 0$ . Besides this we found that the data on the elastic  $pp$  and  $\bar{p}p$  scattering at high energies can be reproduced with a high quality in a model with the dipole pomeron, which has a unit intercept,  $\alpha_{\mathcal{P}}(0) = 1$ , leading to an intermediate growth of the total cross-sections,  $\sigma_{\text{tot}}(s) \propto \ln s$  when  $s \rightarrow \infty$ . Finally, a zero at small  $|t|$  is revealed in the real part of the even amplitude, in agreement with a high energy theorem by Martin.

*Acknowledgements.* We are indebted to E. Predazzi for his support and discussions. Two of us (MG and EM) would like to thank the Dipartimento di Fisica Teorica of the University of Torino for kind hospitality. EM thanks also the Institut de Physique Nucléaire de Lyon for the hospitality. Financial support by the INFN and the MURST of Italy and from the IN2P3 of France is gratefully acknowledged.

## References

1. E.M. Levin, L.L. Frankfurt, Pisma ZhETP, **3**, 105 (1965); H.J. Lipkin, F. Scheck, Phys. Rev. Lett. **16**, 71 (1966); J.J.J. Kokkedee, L. Van Hove, Nuovo Cim. A **42**, 711 (1966)
2. P. Desgrolard, M. Giffon, E. Martynov, E. Predazzi, Eur. Phys. J. C **9**, 623 (1999)
3. T.T. Chou, C.N. Yang, Phys. Rev. **170**, 1591 (1968); Phys. Rev. Lett. **20**, 1213 (1968); Phys. Rev. D **17**, 1889 (1978); C. Bourrely, J. Soffer, T.T. Wu, Phys. Rev. D **19**, 3249 (1979); Nucl. Phys. B **247**, 15 (1984); C. Bourrely, in Elastic and Diffractive Scattering at the Collider and beyond, 1st International Conference on Elastic and Diffractive Scattering, Chateau de Blois, France (1st “Blois workshop”), June 1985, edited by B. Nicolescu, J. Tran Thanh Van (Editions Frontières, 1986) p. 239; L.L. Jenkovszky, B.V. Struminsky, A.N. Wall, Sov. J. Part. Nucl. **19**, 180 (1988)
4. P. Desgrolard, M. Giffon, E. Predazzi, Z. Phys. C **63**, 241 (1994)
5. R.J.M. Covolan, J. Montanha, K. Goulios, Phys. Lett. B **389**, 176 (1996)
6. P. Gauron, B. Nicolescu, E. Leader, Nucl. Phys. B **299**, 640 (1988); Phys. Lett. B **238**, 406 (1990)
7. L.L. Jenkovszky, Fortsch. Phys. **34**, 702 (1986); M. Bertini et al., Rivista Nuovo Cim. **19**, 1 (1996) and references therein



8. F. Pereira, E. Ferreira, Phys. Rev. D **59**, 014008 (1998); *ibid.* **61**, 077507 (2000)
9. E. Levin, An introduction to pomerons, DESY 98-120, TAUP 2522/98, e-Print archive: hep-ph/9808486; E. Predazzi, Diffraction: past, present and future, Lectures given at Hadrons VI, Florianopolis, Brazil, March 1998, DFTT 57/98, e-Print archive: hep-ph/9809454
10. P. Desgrolard, M. Giffon, E. Martynov, E. Predazzi, Eur. Phys. J. C **14**, 683 (2000)
11. M. Giffon, E. Martynov, E. Predazzi, Z. Phys. C **76**, 155 (1997); see also [23]
12. P. Desgrolard, A. Lengyel, E. Martynov, Nuovo Cim. A **110**, 251 (1997)
13. P. Desgrolard, M. Giffon, A.I. Lengyel, E. Martynov, Nuovo Cim. A **107**, 637 (1994)
14. P. Desgrolard, M. Giffon, E. Martynov, Nuovo Cim. A **110**, 537 (1997)
15. M. Block, K. Kang, A.R. White, Mod. Phys. A **7**, 4449 (1992)
16. J.R. Cudell et al., Phys. Rev. D **61**, 034019 (2000)
17. A. Martin, Phys. Lett. B **404**, 137 (1997)
18. P. Desgrolard, A. Lengyel, E. Martynov, Eur. Phys. J. C **7**, 655 (1999)
19. A. Donnachie, P.V. Landshoff, Phys. Lett. B **387**, 637 (1996)
20. A. Donnachie, P.V. Landshoff, Z. Phys. C **2**, 55 (1977); Nucl. Phys. B **231**, 189 (1984); *ibid.* **244**, 322 (1984); *ibid.* **267**, 406 (1986)
21. The data used have been extracted from the PPDS, accessible at <http://pdg.lbl.gov> (computer readable data files)
22. J. Bartels, L.N. Lipatov, G.P. Vacca, Phys. Lett. B **477**, 178 (2000)
23. J. Finkelstein, H.M. Fried, K. Kang, C.-I. Tan, Phys. Lett. B **232**, 257 (1989); E. Martynov, Phys. Lett. B **232**, 367 (1989); H.M. Fried, in Functional Methods and Eikonal Models (Editions Frontières, 1990) p. 214
24. S.B. Nurushev, in Proceedings of the International conference on Elastic and Diffractive Scattering (VIIIth EDS Blois Workshop), Protvino, Russia, 1999, edited by V.A. Petrov, A.V. Prokudin (World Scientific Publishing, 2000) p. 313; S. Weisz, Talk at the International conference on Elastic and Diffractive Scattering (VIIIth EDS Blois Workshop), Protvino, Russia (June 26–July 2, 1999)